Distinctive Thermoresponsive Behavior of Smart Polymers Solvated in Glycerol from Molecular Dynamics

Scott D. Hopkins[a,b] and Estela Blaisten-Barojas[a,b,*]

[a]Center for Simulation and Modeling,
[b]Department of Computational and Data Sciences,
George Mason University, Fairfax, VA 22030, USA, blaisten@gmu.edu

ABSTRACT

Thermoresponsive polymers have been used in a broad range of medical and industrial applications as smart materials, including controlled drug delivery, and water treatment and desalination. While the behavior of such polymers has been modeled in aqueous solutions, study of their behavior in viscous solvents is limited. In this research, the thermoresponsive behavior of PNIPAM and PDEA has been thoroughly evaluated using molecular dynamics techniques and the OPLS/AA force field. Structural and energetic properties including radius of gyration, solvent accessible surface area, and oligomer-solvent interaction energies were characterized. Results indicate that these polymers sustained a coil-to-globule transition in glycerol, with a significant increase in lower critical solution temperature (LCST) when compared to aqueous solutions. These findings yield crucial insights into industrial applications where polymer phase behavior at higher LCST is advantageous.

Keywords: thermoresponsive polymers, Molecular Dynamics, PNIPAM, PDEA, glycerol

1 INTRODUCTION

As part of a large family of thermoresponsive polymers, poly(N-isopropylacrylamide) (PNIPAM) and poly-(N,N-diethylacrylamide) (PDEA) exhibit a coil-to-globule phase transition above a lower critical solution temperature (LCST). The LCST of a particular polymer depends on the local solvent environment and can be tuned by solution parameters such as co-solvent molar concentrations or pH. There has been a large scientific interest in these polymers regarding biomedical applications. In particular, PNIPAM and PDEA in water solutions have an experimental LCST of approximately 305 K, which is relatively close to body temperature and ideal for potential drug delivery systems. As a result, numerous experimental and computational studies have been performed focusing on the properties of these polymers in aqueous solutions [1, 2, 3], including co-solvents of various salts [4], alcohols [5], and urea [6].

There have been a limited number of studies examining more viscous solvents or their mixture with water. For example, experiments on the effect that various concentrations of either glycerol, erythritol, or xylitol mixed with water had on the LCST of PNIPAM [7]. In the case of glycerol, it was shown that up to 0.75 M of glycerol, the LCST of PNIPAM decreased from 305 K to 303 K. However, a mixed solvents environment differ significantly from pure glycerol. Indeed, at 300 K the viscosity of pure glycerol is approximately 17 times higher than the viscosity of a 0.75 M glycerol/water solution.

In this research, Molecular Dynamics (MD) simulations were implemented to evaluate whether in a pure glycerol solvent, the LCST of PNIPAM continued to decrease, or if it exhibited some different behavior. We also examined PDEA solvated in pure glycerol, though no experimental data exists on its LCST inn pure glycerol. For validation on the protocol strategy for determining the LCST, we additionally performed simulations in water.

2 METHODOLOGY

The chemical structure of the PNIPAM and PDEA monomers and of the glycerol and water molecules is provided in Fig. 1. A 3D model of the polymer monomers was initially constructed using the *Avogadro* chemical editor [8], with which we generated a polymer chain with 30 monomers in the syndiotactic isomeric distribution. Hence, the oligomers (polymer chains) had molecular weights of 3,396.819 u and 3,817.629 u for PNIPAM and PDEA, respectively. We term these oligomers 30-PNIPAM containing 572 atoms and 30-PDEA formed by 662 atoms. The all-atom OPLS/AA force field [9] was used with custom generated atomic charges for the two polymers and for the glycerol molecule. The restrained electrostatic potential (RESP) [10] atomic charges were obtained as described in previous work [11]. The AmberTools 20 [12] utilities *Antechamber* and *prepgen* were used to produce head, middle, and tail monomers maintaining the backbone carbon atoms sp^3 hybridization and redistributing any excess charge. For water, the SPC/E force field was employed.

MD simulations were performed using GROMACS 20.4 [13]. The initial 30-PNIPAM and 30-PDEA syndiotactic oligomer geometries were created using a custom python script for alternating the monomers in the

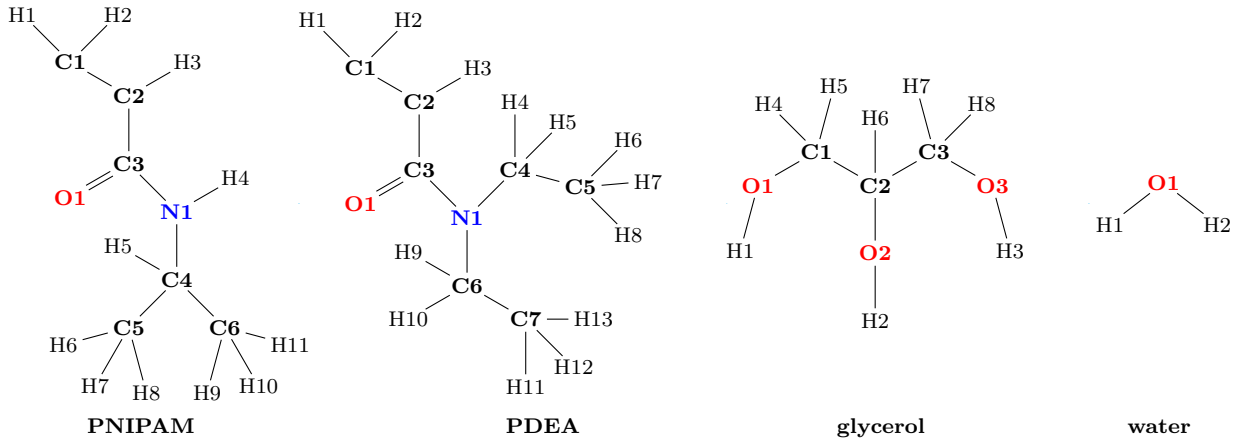

Figure 1: Chemical structure of the PNIPAM and PDEA monomers, the glycerol molecule, and the water molecule.

desired orientation, while the topology files were generated with the aid of the *tppmktop* utility [14]. A similar process was used for establishing the topology file of the glycerol solvent. Simulations were initialized by placing the fully elongated oligomer inside a dodecahedral computational box and solvating with randomly placed solvent molecules, either 2383 glycerol molecules or 10, 980 water molecules. The full system was initially minimized and followed by concatenated NVT and NPT MD simulations to reach equilibration. A collection of temperatures was decided upon between 270 and 400 K and the corresponding equilibration of the system at each of them was achieved over 40 ns NVT-MD followed by NPT-MD runs. The system was equilibrated at 1 atm for all the temperatures considered while fully restraining the oligomer configuration. The Nose-Hoover thermostat and the Parrinello-Rahman pressure coupling were used. In all cases, a 1 fs time step was used for equilibration, periodic boundary conditions and a 1.2 nm cutoff for the electrostatic and van der Waals interactions. The long-range electrostatic interactions were accounted for with the smooth particle-mesh Ewald method (PME) [15] with a Fourier spacing of 0.12 nm. The linear constraint solver LINCS [16] was applied to all bonded hydrogens. To ensure proper statistics of the transition, all production simulations were carried out for 1.0 μs using a time step of 2.0 fs. Reported values were averaged over the last 200 ns of each MD run.

3 RESULTS AND DISCUSSION

The 30-PNIPAM and 30-PDEA systems were simulated at a set of temperatures between 350 and 400 K in glycerol, and between 270 and 320 K in water. The LCST transition temperature for PNIPAM in water was determined to be 298 ± 2 K. This is in agreement with other computational studies and provides confidence in the employed polymer force field. To validate the glycerol model, the equilibrated density of a pure glycerol system was compared to the experimental glycerol density as a function of temperature, and was shown to be in good agreement. In this work we report that the LCST for 30-PNIPAM in glycerol is predicted to occur at 375 ± 4 K, which is a significant increase when compared to the transition in water. This is a novel result, not previously reported in the literature. Similarly for PDEA in pure glycerol, the LCST is predicted at 385 ± 4 K. The following subsections describe structural and energetic analyses performed on the coil and globule phases, while Table 1 summarizes these results.

In general, linear polymers tend to acquire the coil conformation when solvated [11]. Below the LCST temperature, both 30-PINPAM and 30-PDEA display the coil conformation as expected. A coil is a flexible conformation that undergoes continuous bending and twisting with an overall spatially elongated look as shown in Fig. 2 (left). For polymers, the radius of gyration Rg of an oligomer aids in the characterization of the size and compactness acquired by the polymer chain when solvated. Coil conformations are associated to large Rg. Above the LCST transition temperature, thermoresponsive polymers collapse into a globule-like structure with a significantly depleted Rg. Thus, a determination of the Rg is a fingerprint that characterizes the thermoresponsive behavior of polymers. Above the LCST temperature, both 30-PNIPAM and 30-PDEA, displayed a Rg depleted by 40-50 % from the coil phase evidencing the existence of the phase transition in water and in pure glycerol. Figure 2 illustrates the dramatic coil collapse of 30-PINIPAM both, in glycerol and water. Interestingly, in glycerol the globule Rg of 1.19 nm was approximately 16 % higher than the 1.0 nm Rg in water. The glycerol more swollen configuration than in water is possibly due to the larger size of the glycerol molecules that hinder a more compact collapse of the polymer chain. Table 1 summarizes these results.

Another characterization of the coil-to-globule tran-

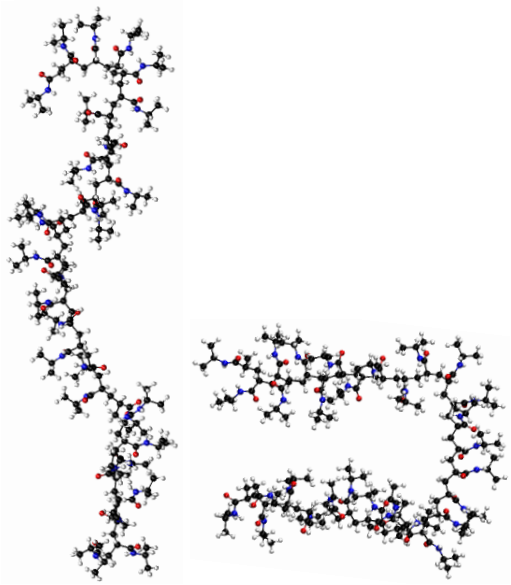

Figure 2: Instantaneous 30-PNIPAM conformation in glycerol in the coil (left) and globule (right) phases along simulations at 370 and 380 K, respectively.

sition was obtained through the analysis of the solvent accessible surface area (SASA), which was determined using the GROMACS *sasa* utility. For 30-PNIPAM in the coil phase, the SASA fluctuated between 39 and 45 nm^2 both in glycerol and in water. Meanwhile in the globule phase, the SASA fluctuations of 34 and 45 nm^2 in glycerol were comparatively larger than the 30 and 38 nm^2 fluctuations observed water. By correlating the SASA with the Rg, the coil and globule phases can be seen more clearly. Figure 3 illustrates this correlation plot and is colored according to the frequency of occurrence with high frequency in red and and low frequency in blue. In glycerol, two distinct high frequency regions are revealed in the globule and coil phases, indicative of two groups of stable configurations. The SASA mean values are listed in Table 1.

From a different perspective, the moments of inertia along the principal axis of the oligomers, I_a, I_b, I_c

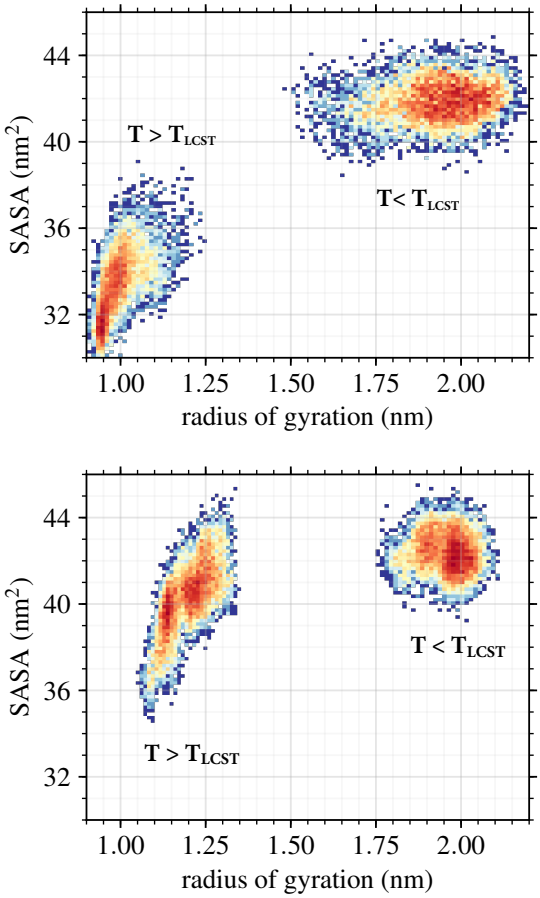

Figure 3: Correlation between the 30-PNIPAM solvent accessible surface area (SASA) and its radius of gyration in water (top) and in glycerol (bottom). Showed is the dramatic change when the system temperature T is above T_{LCST} (left) or below T_{LCST} (right).

were also analyzed. The ratios I_b/I_a and I_c/I_a in the coil phase are approximately 5 to 6 times higher than those in the globule phase emphasizing the appearance of the compact globule conformation above the LCST transition temperature, as shown in Table 1.

Table 1: Property averages and standard deviations. HB and E_{int} are per monomer.

solvent	oligomer	phase	R_g (nm)	SASA (nm^2)	I_b/I_a	$HB_{(CO-HO)}$	$HB_{(NH-OH)}$	E_{int} (kJ/mol)
glycerol	PNIPAM	coil	1.96 ± 0.06	42.3 ± 0.9	12.1 ± 2.9	0.59 ± 0.09	0.50 ± 0.08	-93.7 ± 3.9
		glob.	1.19 ± 0.06	39.6 ± 1.1	1.5 ± 0.3	0.57 ± 0.09	0.47 ± 0.09	-92.3 ± 4.0
	PDEA	coil	1.71 ± 0.09	41.4 ± 0.7	12.0 ± 2.8	0.46 ± 0.09	—	-82.3 ± 3.7
		glob.	1.24 ± 0.04	39.0 ± 0.7	2.2 ± 0.4	0.48 ± 0.08	—	-80.3 ± 3.5
water	PNIPAM	coil	1.95 ± 0.12	41.8 ± 0.9	9.10 ± 4.47	1.75 ± 0.09	0.57 ± 0.09	-100.6 ± 3.3
		glob.	1.00 ± 0.03	33.2 ± 1.3	1.55 ± 0.23	1.54 ± 0.10	0.53 ± 0.09	-90.7 ± 6.2
	PDEA	coil	1.68 ± 0.09	41.9 ± 0.8	6.21 ± 2.62	1.57 ± 0.08	—	-89.7 ± 2.5
		glob.	1.17 ± 0.03	35.5 ± 1.1	2.87 ± 0.44	1.35 ± 0.08	—	-78.0 ± 3.6

The number of hydrogen bonds per monomer, HB, were calculated using the GROMACS *hbond* utility with a hydrogen-donor-acceptor cutoff angle of 30 degrees and a donor-acceptor cutoff distance of 0.35 nm. Both in water and glycerol, hydrogen bonds are formed between the oligomer and the solvent, as well as between intra-oligomer monomers. For 30-PNIPAM, hydrogen bonds occur between the carbonyl oxygen of the oligomer and hydroxyl hydrogen of the solvent, HB_{CO-HO}, and between the amine hydrogen of the oligomer and the hydroxyl oxygen of the solvent, HB_{NH-OH}, as reported in Table 1. A small number of monomer-monomer hydrogen bonds are also present between the carbonyl oxygen and amine hydrogen. While the oligomer-solvent hydrogen bonds frequency decreased slightly above the LCST, the monomer-monomer HB frequency increased slightly.

The interaction energy between the oligomer and solvent, E_{int}, was determined via the GROMACS *rerun* command that analyzed the Lennard-Jones and Coulomb potential energy between all oligomer and solvent atoms. For the water system below the LCST, the 30-PNIPAM E_{int} per monomer was approximately -100 kJ/mol, while above the LCST it was approximately -91 kJ/mol. This increase in interaction energy indicates a less favorable system state, leading to a decrease in solubility. In the glycerol system, the interaction energy was the same above and below the LCST, at approximately -93 kJ/mol.

4 CONCLUSION

Based on extensive Molecular Dynamics simulations, this research predicts that 30-PNIPAM and 30-PDEA syndiotactic oligomers undergo a coil-to-globule transition when solvated in glycerol. The predicted LCST temperatures around 370-380 K for both oligomers in glycerol occur at approximately 80 K higher than when in either pure water or in aqueous glycerol solutions with up to 0.75 M glycerol. At the predicted LCST transition temperatures, the viscosity of glycerol is approximately 0.014 Ns/m^2, compared to 0.510 Ns/m^2 at 304 K. For comparison, a 0.75 M glycerol/water solution at 304 K has a viscosity of 0.030 Ns/m^s. This dramatic decrease in viscosity at high temperatures most likely enables the reappearance of a LCST in a pure glycerol solvent.

Since the predicted LCST of PNIPAM and PDEA in glycerol are above the boiling point of water, glycerol is a candidate solvent for industrial applications where polymer phase change behavior at higher temperatures would be advantageous.

ACKNOWLEDGEMENT

Simulations were performed on the high performance computing clusters of the Office of Research Computing at George Mason University.

REFERENCES

[1] Y. Kang, H. Joo, and J. S. Kim, Collapse-swelling transitions of a thermoresponsive, single poly(N-isopropylacrylamide) chain in water, *J. Phys. Chem. B*, 120, 13184-13192, 2016.

[2] C. Dalgicdir and N. F. A. van der Vegt, Improved temperature behavior of PNIPAM in water with a modified OPLS model, *J. Phys. Chem. B,* 123, 3875-3883, 2019.

[3] X. Pang and S. Cui, Single-chain mechanics of poly(N,N-diethylacrylamide) and poly(n-isopropylacrylamide): Comparative study reveals the effect of hydrogen bond donors, *Langmuir*, 29, 12176-12182, 2013.

[4] H. Du, R. Wickramasinghe, and X. Qian, Effects of salt on the lower critical solution temperature of poly (N-isopropylacrylamide), *J. Phys. Chem. B*, 114, 16594-16604, 2010.

[5] H. A. Pérez-Ramrez, C. Haro-Pérez, and G. Odriozola, Effect of temperature on the cononsolvency of poly(N-isopropylacrylamide) (PNIPAM) in aqueous 1-propanol, *ACS Appl. Polym. Mater.*, 1, 2961-2972, 2019.

[6] S. Micciulla, J. Michalowsky, M. A. Schroer, C. Holm, R. V. Klitzing, and J. Smiatek, Concentration dependent effects of urea binding to poly(N- isopropylacrylamide) brushes: A combined experimental and numerical study, *Phys. Chem. Chem. Phys.,* 18, 5324-5335, 2016.

[7] P. Narang and P. Venkatesu, Unravelling the role of polyols with increasing carbon chain length and OH groups on the phase transition behavior of PNIPAM, *New J. Chem.*, 42, 13708-13717, 2018.

[8] M. D. Hanwell and et al., Avogadro: An advanced semantic chemical editor, visualization, and analysis platform, *J. Cheminf.*, 4, 2012. DOI: 10.1186/1758-2946-4-17.

[9] W. L. Jorgensen, D. S. Maxwell, and J. Tirado-Rives, Development and testing of the OPLS all-atom force field on conformational energetics and properties of organic liquids, *J. Am. Chem. Soc.*, 118, 11225-11236, 1996.

[10] J. Wang, W. Wang, P. A. Kollman, and D. A. Case, Automatic atom type and bond type perception in molecular mechanical calculations, *J. Mol. Graphics Model.*, 25, 247-260, 2006.

[11] S. D. Hopkins, G. Gogovi, E. Weisel, R. A. Handler, and E. Blaisten-Barojas, Polyacrylamide in glycerol solutions from an atomistic perspective of the energetics, structure, and dynamics, *AIP Advances*, 10, 08501, 2020.

[12] Amber 2020 Manual, Covers Amber20 and AmberTools20, https://ambermd.org/doc12/Amber20.pdf. (accessed 15 April, 2022).

[13] M. Abraham, D. van der Spoel, E. Lindahl, B. Hess, et al., GROMACS User Manual 2020, 2020, https://manual.gromacs.org/documentation/2020/manual-2020.pdf, (accessed 15 April, 2022).

[14] TPPMKTOP Database, ERG Research Group, 2015, http//erg.biophys.msu.ru/tpp, (accessed 15 April, 2022).

[15] U. Essmann, L. Perera, M. L. Berkowitz, T. Dar- den, H. Lee, and L. G. Pedersen, A smooth particle mesh Ewald method, *J. Chem. Phys.*, 103, 8577, 1995.

[16] B. Hess, H. Bekker, H. J. Berendsen, J. G. Fraaije, LINCS: A Linear Constraint Solver for molecular simulations, *J. Comput. Chem.*, 18, 1463-1472, 1997.